SLAC–PUB–6208
May 1993
(A)

Beam Dispersion Measurements with Wire Scanners in the SLC Final Focus Systems*

P. Emma, D. McCormick, M.C. Ross
Stanford Linear Accelerator Center
Stanford, California 94309

ABSTRACT

A method is described to make a direct measurement of the horizontal and vertical momentum dispersion of the electron and positron beams as they pass through the chromatic correction sections (CCS) of the SLC final focus systems. The method is advantageous since it cleanly separates betatron components of the beam size from dispersive components, can be measured during standard colliding beams machine conditions in a minute or two, and directly measures the energy-position correlation within the beam.

I. INTRODUCTION

A dispersion measurement in circular accelerators usually requires sampling an off-energy orbit with beam position monitors. The cyclic boundary conditions provide a closed dispersion function which is measurable by observing the beam centroid. In linear colliders, however, varying the beam energy at some point in the beam line and observing downstream beam centroid positions measures the position/energy transfer matrix element (*e.g.* R_{16}) from the point of energy change to the orbit observation point. If a dispersion source exists upstream of the energy variation point, its contribution to the total dispersion function will not be measured. Since it is usually important to remove all energy-position correlations to minimize the transverse beam size, a beam centroid based correction technique as used in circular machines may not fully correct the total beam dispersion. Furthermore, other sources of beam energy spread (*e.g.* synchrotron radiation in the SLC collider arcs) produce energy-position beam correlations[1] which are not measured with a simple beam centroid observation technique.

In the SLC final focus, residual dispersion at the interaction point (IP) has normally been corrected by varying the beam energy at the end of the linac and setting quadrupoles of the final focus dispersion matching section to cancel the correlated transverse beam motion at the beam position monitors[2] (BPM). Because of the strong magnification of the sine-like betatron phase in the final focus and the demagnification of the cosine-like phase, the resolution of the angular IP dispersion, η'^* (sine-like), using the BPMs is very good, but the resolution of the spatial IP dispersion, η^* (cosine-like), is very poor. Therefore, η^* is actually corrected by minimizing the IP beam size with closed trajectory bumps in the sextupoles of the CCS, or more recently, with four small CCS correction quadrupoles[3]. Unfortunately, the BPM method actually corrects the R_{26} transfer matrix element from linac to IP and the R_{26} is not necessarily equal to the total IP energy-angle correlation, η'^*.

The actual η'^*, and a finite beam energy spread, produces larger angular divergence at the IP (larger beam size at the final triplet) which may increase detector backgrounds through bremstrahlung of the more intense focusing. In order to compensate for increased detector backgrounds the total divergence must be reduced with upstream final focus beta matching quadrupoles. This divergence reduction has the undesirable effect of increasing the beam size at the IP (increase of β^*). For this reason the actual η'^* must be minimized. Therefore it is useful to find a fast, direct method to measure the energy-position correlations in the beam which are present under normal machine operating conditions.

II. APPLICATION TO THE SLC

The most useful place to measure the total accumulated beam dispersion in the SLC is in the final focus just before the beams are squeezed down to transverse sizes of ~2 μm. In order to provide separation of betatron beam size components from dispersive components some section with bending is necessary. The nominal bending and optical symmetries of the final focus CCS (Fig 1) are ideal for this purpose.

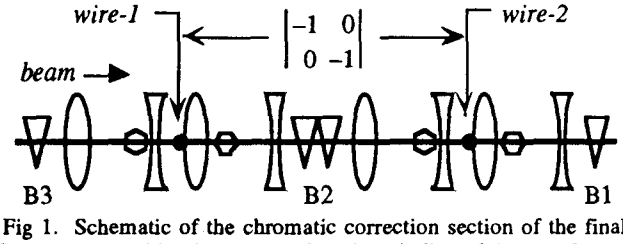

Fig 1. Schematic of the chromatic correction section of the final focus system with wire scanner locations indicated (sextupoles are drawn as hexagons). The interaction point (not shown) is located downstream of bend B1 by a betatron phase advance of π.

Wire scanners at the two points in the CCS where the horizontal dispersion is a maximum are used to compare the beam sizes at these two locations. In order to cancel geometric aberrations, the 4×4 linear transfer matrix between nested sextupole pairs is $-I$. This $-I$ matrix between the first wire scanner (*wire-1* in Fig 1) and second wire scanner (*wire-2*) ensures equal beta functions at the two wires.

$$\beta_{x1} = \beta_{x2} \equiv \beta_x , \quad \beta_{y1} = \beta_{y2} \equiv \beta_y \tag{1}$$

Propagating the horizontal dispersion function from wire-1 to wire-2 yields

$$\eta_{x1} + \eta_{x2} = R_{16} \equiv 2\bar{\eta}_x , \tag{2}$$

where the transfer matrix element R_{16} (=540 mm) from wire-1 to wire-2 is solely defined by the local lattice (B2 horizontal bending dipoles in Fig 1). Similarly, an incoming

* Work supported by Department of Energy contract DE-AC03-76SF00515

Presented at the Particle Accelerator Conference (PAC 93), Washington, D.C., May 17-20, 1993.

mismatched component of the dispersion function, $\Delta\eta$, including all upstream sources of position-energy correlation, will propagate freely through the final focus.

$$\Delta\eta_{x1,y1} = -\Delta\eta_{x2,y2} \equiv \Delta\eta_{x,y} \tag{3}$$

Here $\Delta\eta_{xi,yi}$ is the residual spatial component of the dispersion at wire-i.

These beta and dispersion functions contribute to the beam sizes at the wire scanners in different ways. Writing the transverse position of a particle at each wire location, using the $-I$ matrix between them, and expressing the random fractional energy deviation as $\delta \equiv \delta E/E$ ($=\delta p/p$ for these ultra-relativistic electrons/positrons) yields

$$\begin{aligned} x_1 &= \ x_\beta + (\bar{\eta}_x + \Delta\eta_x)\delta \\ x_2 &= -x_\beta + (\bar{\eta}_x - \Delta\eta_x)\delta \\ y_1 &= \ y_\beta + \Delta\eta_y\delta \\ y_2 &= -y_\beta - \Delta\eta_y\delta \end{aligned} \quad , \tag{4}$$

where x_β, y_β are betatron position components at wire-1 which reverse sign through the $-I$ transfer to wire-2. These betatron components may also be expressed in terms of the transverse beam emittances, ε_x and ε_y (all random variables throughout are assumed to have zero mean).

$$\langle x_\beta^2 \rangle \equiv \varepsilon_x\beta_x \ , \qquad \langle y_\beta^2 \rangle \equiv \varepsilon_y\beta_y \tag{5}$$

Since $\Delta\eta_{x,y}$ includes all position-energy correlations, then by definition x_β and y_β will not be correlated with δ (*i.e.* $\langle x_\beta\delta\rangle = \langle y_\beta\delta\rangle = 0$). The beam sizes at the wires are then

$$\langle x_1^2 \rangle = \varepsilon_x\beta_x + (\bar{\eta}_x^2 + 2\bar{\eta}_x\Delta\eta_x + \Delta\eta_x^2)\langle\delta^2\rangle \ , \tag{6}$$

$$\langle x_2^2 \rangle = \varepsilon_x\beta_x + (\bar{\eta}_x^2 - 2\bar{\eta}_x\Delta\eta_x + \Delta\eta_x^2)\langle\delta^2\rangle \ , \tag{7}$$

$$\langle y_1^2 \rangle = \varepsilon_y\beta_y + \Delta\eta_y^2\langle\delta^2\rangle = \langle y_2^2 \rangle . \tag{8}$$

From the difference of (6) and (7), and knowledge of the beam energy spread, comes the mismatched component of the horizontal dispersion, $\Delta\eta_x$. However, the vertical beam sizes at wire-1 and wire-2 are always equal (8) since there is no vertical bending between wires. So measurement of the vertical beam profile is not as useful to measure dispersion. The vertical dispersion can, however, be measured by observing the X-Y coupling it generates in the presence of the nominal horizontal dispersion. The X-Y coupling is measured by taking advantage of the 3-wire orientations of the available SLC wire scanners[4]. The best resolution of $\Delta\eta_{x,y}$ is achieved using a horizontal scan direction (given wire orientations on the support fork of Fig 2).

The leftmost wire in Fig 2 (*U-wire*) scans the beam profile along $u = (x + y)/\sqrt{2}$. The rightmost wire (*V-wire*) scans along $v = (x - y)/\sqrt{2}$. All other SLC wire scanner installations are rotated 45 degrees to Fig 2 such that X, Y, and U beam profile scans are made[4].

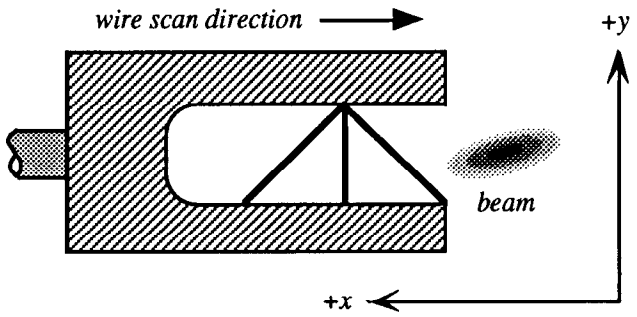

Fig 2. Horizontally installed SLC wire scanner viewed in the beam direction. Leftmost wire is the *U-wire*, center is the *X-wire*, and rightmost is the *V-wire*.

With this horizontal scan direction, the beam profile is measured along the X-axis, as well as the U and V-axis.

$$\langle u^2 \rangle = \frac{1}{2}\left(\langle x^2 \rangle + \langle y^2 \rangle\right) + \langle xy \rangle \tag{9}$$

$$\langle v^2 \rangle = \frac{1}{2}\left(\langle x^2 \rangle + \langle y^2 \rangle\right) - \langle xy \rangle \tag{10}$$

From (4), the X-Y coupling term at each wire is

$$\langle x_1y_1 \rangle = \langle x_\beta y_\beta \rangle + \Delta\eta_x\Delta\eta_y\sigma_\delta^2 + \bar{\eta}_x\Delta\eta_y\sigma_\delta^2 \ , \tag{11}$$

$$\langle x_2y_2 \rangle = \langle x_\beta y_\beta \rangle + \Delta\eta_x\Delta\eta_y\sigma_\delta^2 - \bar{\eta}_x\Delta\eta_y\sigma_\delta^2 \ , \tag{12}$$

with $\langle x_\beta y_\beta \rangle$ as the observable phase of the betatron component of X-Y coupling, and $\sigma_\delta^2 = \langle\delta^2\rangle$. Using (6) through (12) yields an over determined linear system relating the discernible beam size components to the six measured beam profiles at the two wires.

$$\begin{pmatrix} \sigma_{x1}^2 \\ \sigma_{u1}^2 \\ \sigma_{v1}^2 \\ \sigma_{x2}^2 \\ \sigma_{u2}^2 \\ \sigma_{v2}^2 \end{pmatrix} = \begin{pmatrix} 1 & 1 & 0 & 0 & 0 \\ .5 & .5 & .5 & 1 & 1 \\ .5 & .5 & .5 & -1 & -1 \\ 1 & -1 & 0 & 0 & 0 \\ .5 & -.5 & .5 & 1 & -1 \\ .5 & -.5 & .5 & -1 & 1 \end{pmatrix} \times \begin{pmatrix} \varepsilon_x\beta_x + \left(\bar{\eta}_x^2 + \Delta\eta_x^2\right)\sigma_\delta^2 \\ 2\bar{\eta}_x\Delta\eta_x\sigma_\delta^2 \\ \varepsilon_y\beta_y + \Delta\eta_y^2\sigma_\delta^2 \\ \langle x_\beta y_\beta \rangle + \Delta\eta_x\Delta\eta_y\sigma_\delta^2 \\ \bar{\eta}_x\Delta\eta_y\sigma_\delta^2 \end{pmatrix} \tag{13}$$

The spatial components of the mismatched dispersion are then

$$\Delta\eta_x = \frac{\left(2\sigma_{x1}^2 + \sigma_{u1}^2 + \sigma_{v1}^2 - 2\sigma_{x2}^2 - \sigma_{u2}^2 - \sigma_{v2}^2\right)}{12\bar{\eta}_x\sigma_\delta^2} \ , \tag{14}$$

$$\Delta\eta_y = \frac{\left(\sigma_{u1}^2 - \sigma_{v1}^2 - \sigma_{u2}^2 + \sigma_{v2}^2\right)}{4\bar{\eta}_x\sigma_\delta^2} \ , \tag{15}$$

where the notation σ^2 has replaced expectation brackets and the energy spread, σ_δ, must be known from other measurements. In practice, a weighted fit using (13) and the measurement errors is employed.

III. Resolution and Errors

For reasons described in the introduction, a tolerance may be specified on η'^*. The present background limited IP divergence, $\hat{\sigma}_\theta$, is 300-350 μrad rms. Given typical SLC IP energy spread, σ_δ, of ~0.2% rms, a tolerance on $|\eta'^*|$ of ≤50 mrad limits the related transverse IP beam size increase, σ_{IP}/σ_{IP0}, to ≤5%.

$$\frac{\sigma_{IP}}{\sigma_{IP0}} = \frac{\hat{\sigma}_\theta}{\sqrt{\hat{\sigma}_\theta^2 - \eta'^{*2}\sigma_\delta^2}} \leq 1.05 \qquad (16)$$

Due to the $n\pi + \pi/2$ (n = 1,2) betatron phase advance from the CCS wire scanners to the IP, $\Delta\eta_{x,y}$ at wire-1 translates into $\eta'^*_{x,y}$ through the R_{12} (=−3.2 m) and R_{34} (=−1.2 m) matrix elements from wire-1 to IP.

$$\eta_x'^* = \frac{\Delta\eta_x}{R_{12}} \quad , \quad \eta_y'^* = \frac{\Delta\eta_y}{R_{34}} \qquad (17)$$

The resolution of the IP angular dispersion from (14), (15), and (17) is

$$\sigma_{\eta_x'^*} = \frac{\sigma_R\sqrt{4\sigma_x^2 + \sigma_u^2 + \sigma_v^2}}{3\sqrt{2}\,R_{12}\bar{\eta}_x\sigma_\delta^2} , \qquad (18)$$

$$\sigma_{\eta_y'^*} = \frac{\sigma_R\sqrt{\sigma_u^2 + \sigma_v^2}}{\sqrt{2}\,R_{34}\bar{\eta}_x\sigma_\delta^2} , \qquad (19)$$

with σ_R as the CCS wire scanner instrumental resolution (~50 μm), and σ_x, σ_u, and σ_v as the measured beam profiles at the wires (in this case assumed equal at both wires for simplicity). From the approximate SLC CCS beam parameters

$$\begin{array}{ll} \beta_x = 2000 \text{ m} & \beta_y = 300 \text{ m} \\ \varepsilon_x = 600 \text{ μm-μrad} & \varepsilon_y = 400 \text{ μm-μrad} \\ \sigma_\delta = 0.2\ \% & \bar{\sigma}_x = 1.2 \text{ mm} \\ \sigma_u = \sigma_v = 0.9 \text{ mm} & \bar{\eta}_x = 270 \text{ mm} \end{array} \qquad (20)$$

and assuming matched conditions and no large betatron X-Y coupling, the resolutions from (18) and (19) are

$$\begin{aligned} \sigma_{\eta_x'^*} &= 9 \text{ mrad } (\ll 50 \text{ mrad}) , \\ \sigma_{\eta_y'^*} &= 35 \text{ mrad } (<50 \text{ mrad}) . \end{aligned} \qquad (21)$$

The horizontal dispersion resolution is more than sufficient, however the vertical resolution is just adequate. Allowing for poorly matched conditions, coupling, and reasonably larger emittances produces resolutions which may increase by up to a factor of 2. Several repeated measurements, as the matching is improved, may be necessary in this case.

A systematic mis-scaling between the two wire scanners of 5%, given actual matched conditions (20), produces a tolerable 10 mrad apparent $\eta_x'^*$. This same mis-scaling produces no error for $\eta_y'^*$. An achievable relative roll error between wire-1 and wire-2 of ≤1° produces an apparent $|\eta_y'^*|$ of ≤8 mrad.

Turtle[5] tracking calculations have shown no significant systematic error in the measurement of $\eta'^*_{x,y}$ produced by local sextupole aberrations (<1 mrad), or by full scale tuning of the nearby IP dispersion correction quadrupoles (<8 mrad).

IV. Correction Scheme

The actual correction algorithm requires a scan of the CCS wires, and the use of (13) and (17) to fit for $\eta'^*_{x,y}$. Next the X and Y beam sizes at the IP are minimized with the small CCS correction quadrupoles (using beam-beam deflections[6] to measure the beam sizes) and these quadrupole settings are used to calculate the existing residual $\eta^*_{x,y}$. The values of residual angular and spatial IP dispersion are then back-propagated to the final focus dispersion matching section (upstream of the CCS). A non-linear fitting program is then used to calculate the new settings of the dispersion matching section quadrupoles in order to cancel the residual angular and spatial IP dispersion (assuming the mismatched dispersion is not generated within the final focus), and the CCS correction quadrupoles are reset to zero. The IP beam sizes are finally minimized one more time with the CCS correction quadrupoles to fine tune the beam.

With the residual dispersion corrected at the wires, (13) may also be used to fit for the betatron X-Y coupling term, $\langle x_\beta y_\beta \rangle$, which would otherwise be improperly measured in the presence of significant residual dispersion.

V. Acknowledgments

The authors are grateful to Eric Bong for mechanical support in the design and installation of the wire scanner hardware and Nick Walker and Pantaleo Raimondi for many useful discussions. We are also grateful to Leeanne Yasukawa and Linda Hendrickson for software support.

VI. References

[1] W. Spence, *Private Communication.*

[2] C.M. Hawkes and P.S. Bambade, "First Order Optical Matching in the Final Focus Section of the SLAC Linear Collider", *Nucl. Inst. and Meth.* **A274** (1989) 27.

[3] P. Emma, "Minimizing Residual Dispersion at the SLC Interaction Point", (to be published)

[4] M.C. Ross, *et.al.*, "Wire Scanners for Beam Size and Emittance Measurement at the SLC", Proceedings of the 1991 IEEE Particle Accelerator Conference, p.1201, May 1991

[5] D.C. Carey, K.L. Brown, Ch. Iselin, "Decay Turtle", SLAC-246, March 1982.

[6] P. Bambade, *et.al.*, "Observation of Beam-Beam Deflections at the Interaction Point of the SLAC Linear Collider", *Physical Review Letters*, Vol 62, No 25, p 2949, June 1989.